Properties of X-Ray Afterglows of Gamma-Ray Bursts

Rie Sato

Tokyo Institute of Technology

Outline

Properties of Gamma-ray bursts (GRBs)

- Swift detected 160 GRBs during 2005/01-2006/09.
- Systematic analysis of 160 prompt emissions

Properties of the early X-ray afterglows

- Systematic analysis of 128 X-ray afterglows:
  Properties of rapid decay, shallow decay, X-ray flares
- Identification of rapid decay phase
- Properties of the X-ray flares
- Relation of the shallow decay phase and prompt emission

Gamma-Ray Bursts

Gamma-ray bursts (GRBs) are

- the most energetic explosions in the universe.
- at the cosmological distances (average redshift: z~1.3).
- At least some GRBs are associated with supernova explosions.

Afterglows are

- broad-band (radio/infrared /optical/X-ray).
- Most lightcurves show a smooth power-law decay with the time ($\propto t^{-1}$).

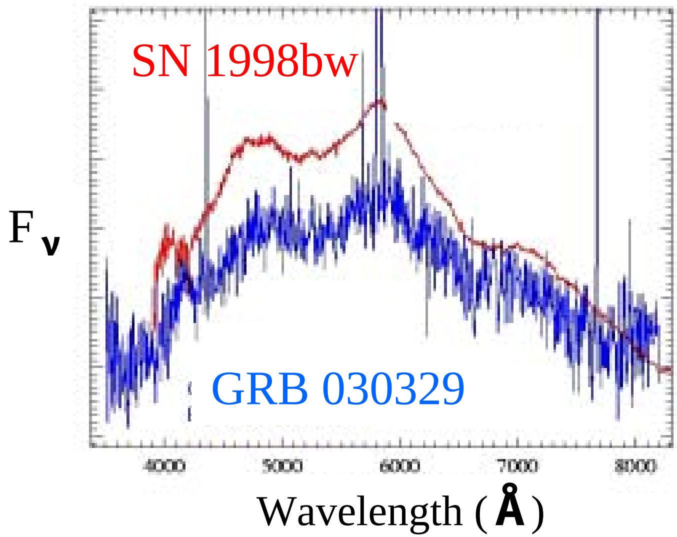

The afterglow spectrum of GRB 030329 reveals the spectral signature of Type-Ib/c supernova.

Radiation mechanism of GRBs

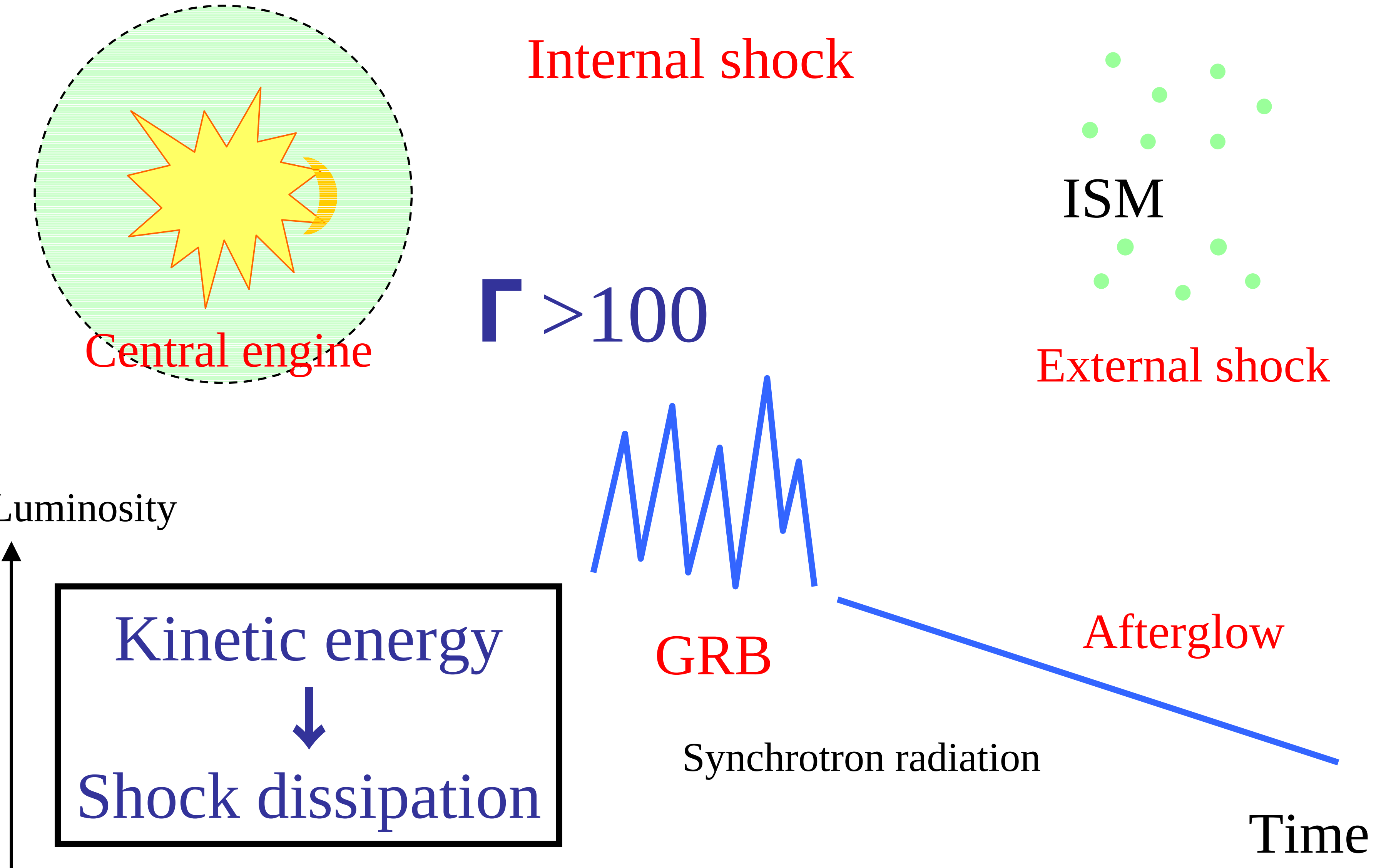

Afterglow observation

Afterglows provide

- accurate GRB position
- redshift
- GRB jet structure
- energy balance

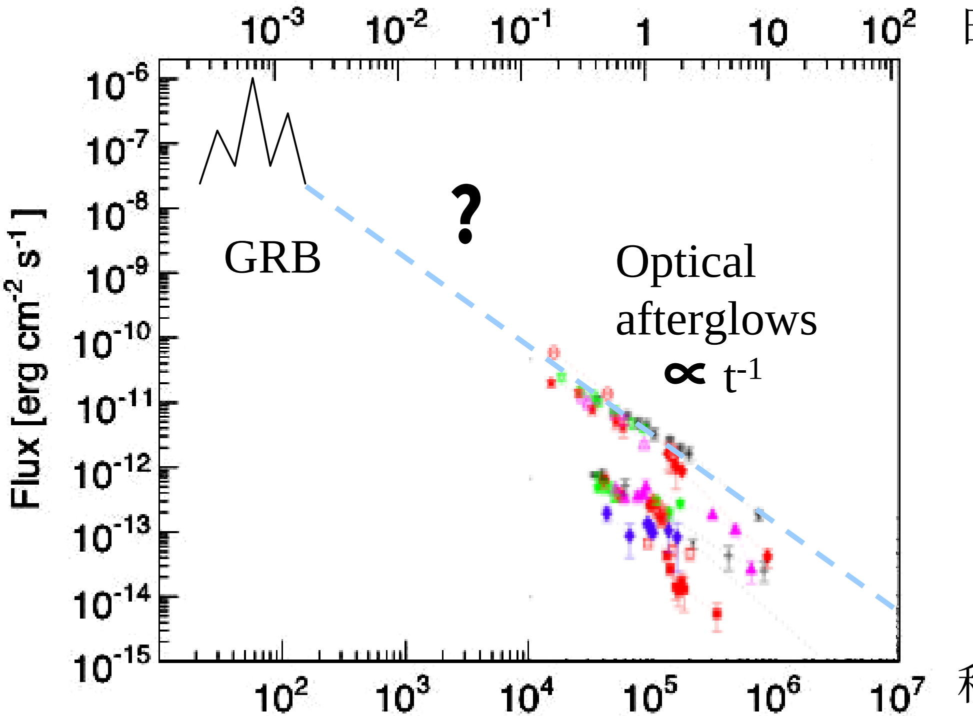

Genre & Boer 2005

What is the connection between the GRB and the afterglow ?
Simple power-law function ?

Light curves of the early optical afterglows

However,
some optical afterglows show deviations from a smooth power-law.

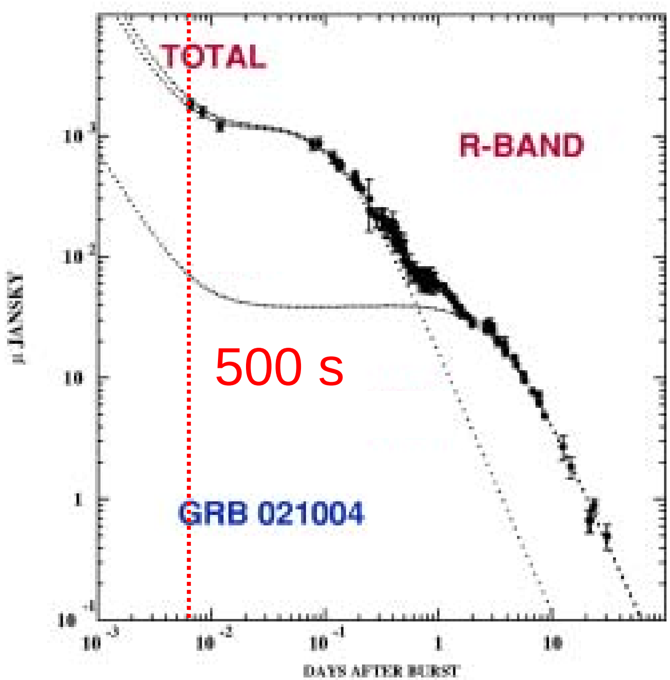

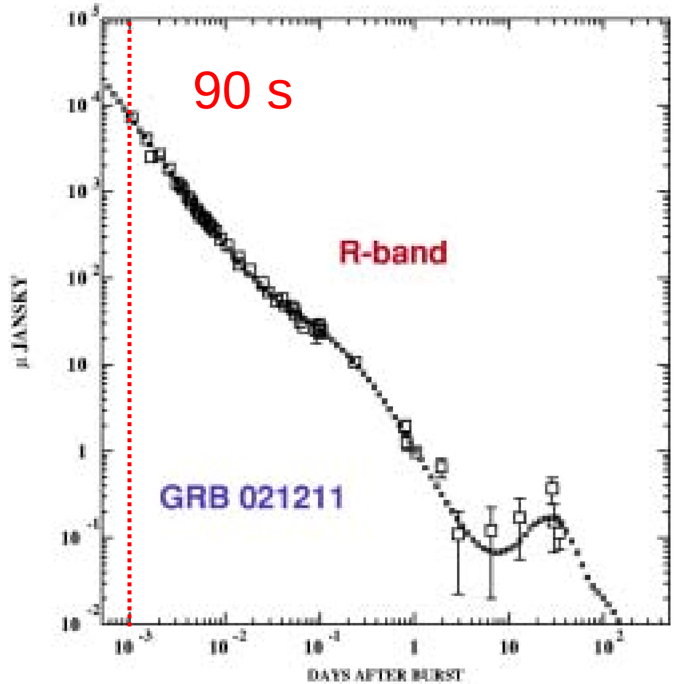

- Shallow decay phase was observed in the early optical light curve.
- Steep decay was observed in the early optical light curve.
  (Bump was observed in the late time (1 day~).)

Swift

Swift is the first mission with ability to begin multi-wavelength observations within ~1 min after the detection of GRBs

Launched in 2004/11/20

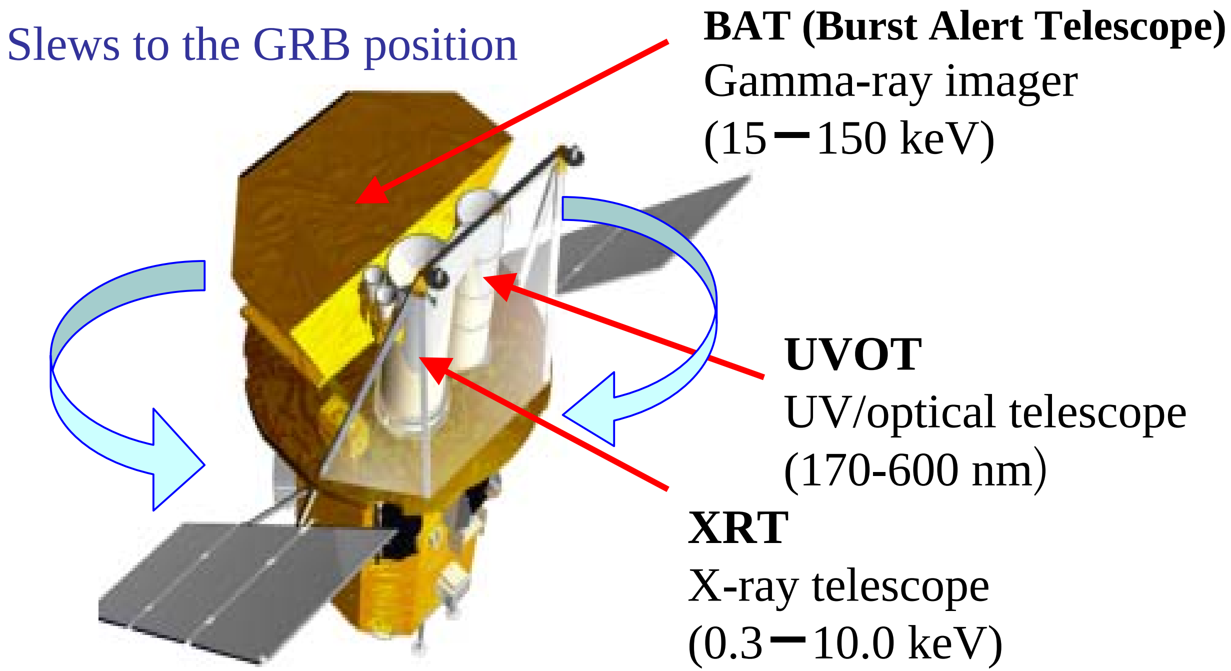

Swift makes it possible to perform follow-up observations within 100 s after the bursts.

Delta II ~600 km ~21°

Swift GRBs

Temporal studies

Light curves in the energy range of 15-150 keV

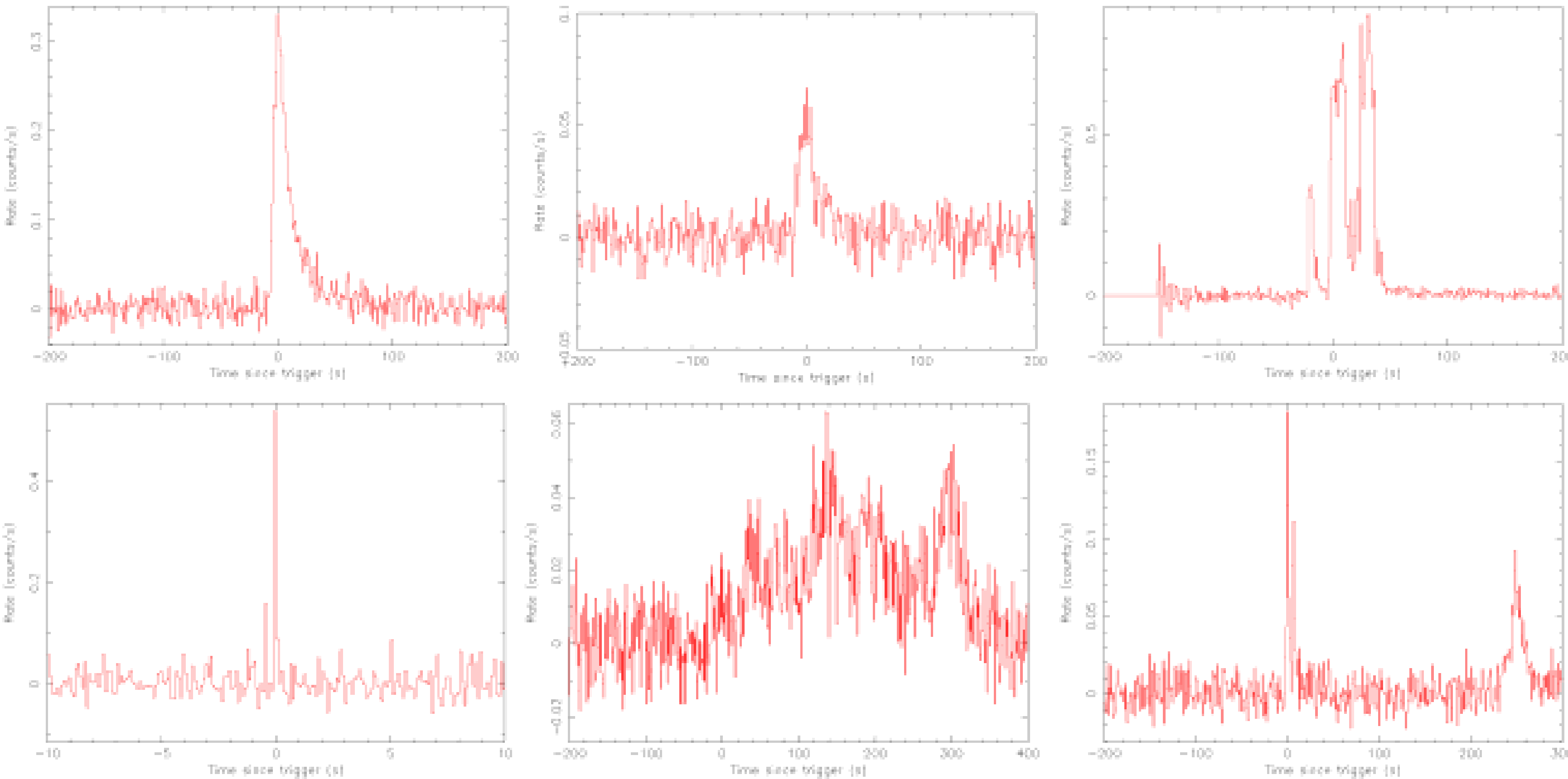

Burst duration

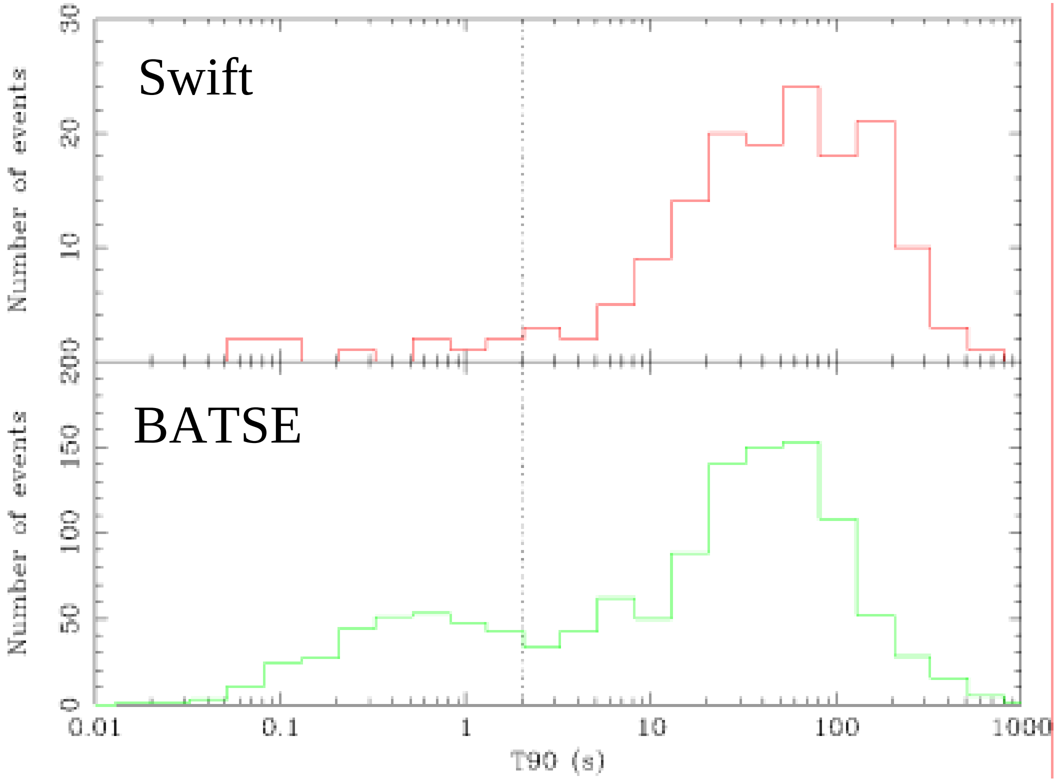

- Duration are distributed around 10-100 s.
- Swift GRBs do not show clear "bimodal" distribution.

Differences of the energy band and trigger system ?

Spectral studies

Systematic analysis of 160 prompt emissions (2005/01-2006/09)

- Typical GRB → Band function Γ_1~-1, Γ_2~-2.2, E_p~250 keV
- Best fit models of BAT spectra (15-150 keV)
  134 GRBs : single power-law (photon index ~ -1.5)
  26 GRBs : cutoff power-law
- For six GRBs which obtained both redshift and E_p follow the $E_p \propto E_{iso}^{0.5}$ and $L_p \propto E_p^{2.0}$ re

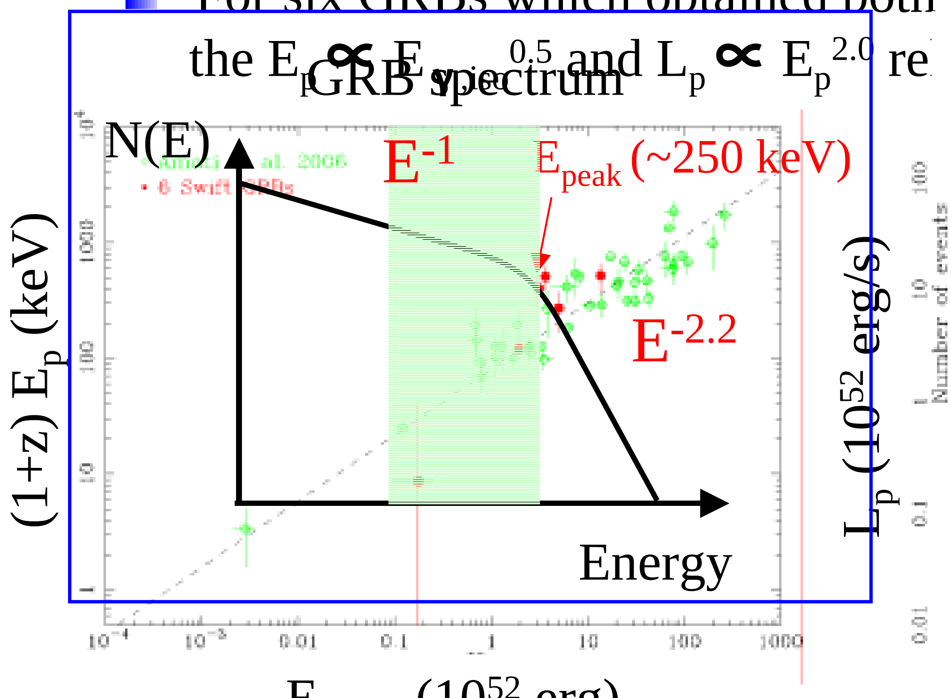

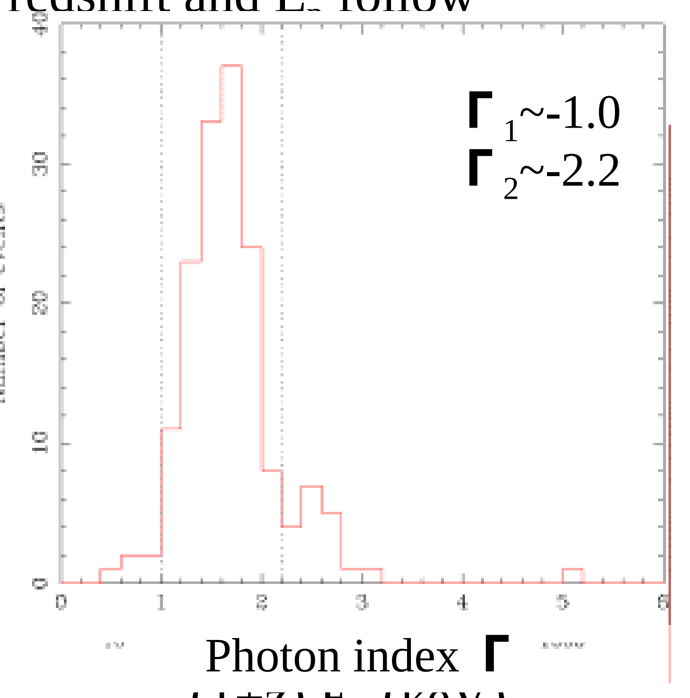

X-ray afterglows

Light curves

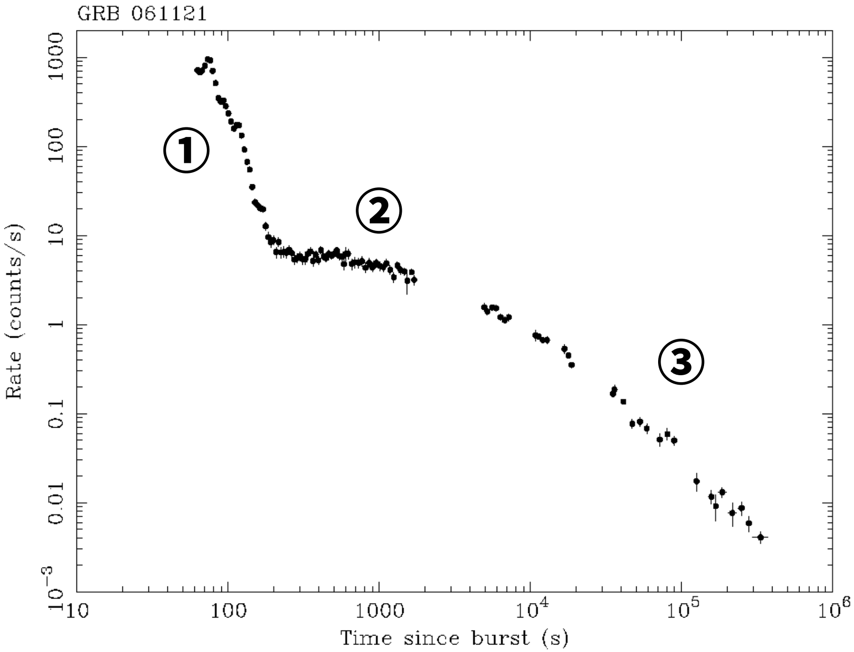

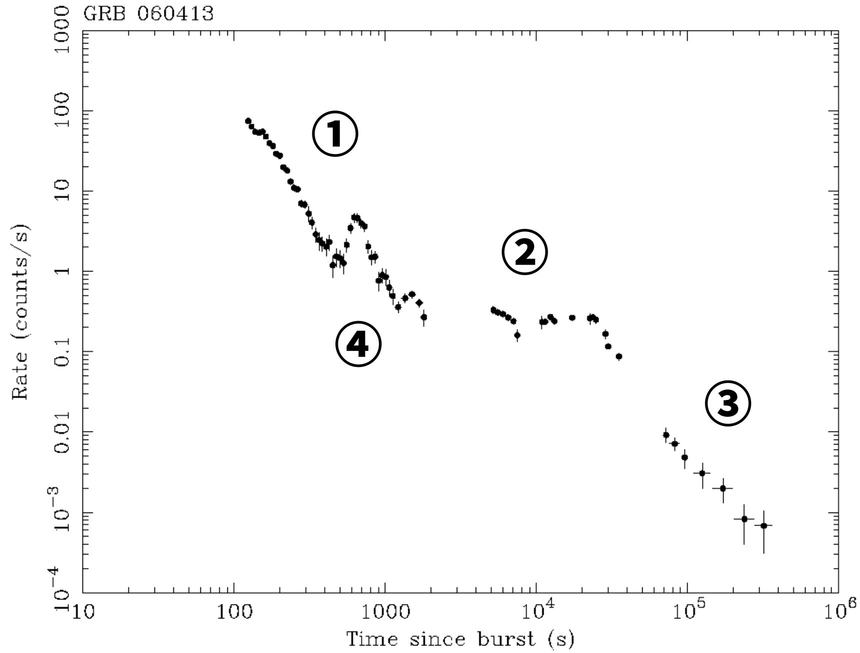

Light curves of X-ray afterglows show three distinct power-law segments.

① initial steep decay phase (α_1 ~ -3)

② very shallow decay phase (α_2 ~ -0.5)

③ steeper decay phase (α_3 ~ -1)

④ X-ray flares

Rapid decay

Curvature effect

The prompt emission from the large angles ($\theta > \Gamma^{-1}$) that reaches observer at late time ($\Delta t \sim R\theta^2/2c$).

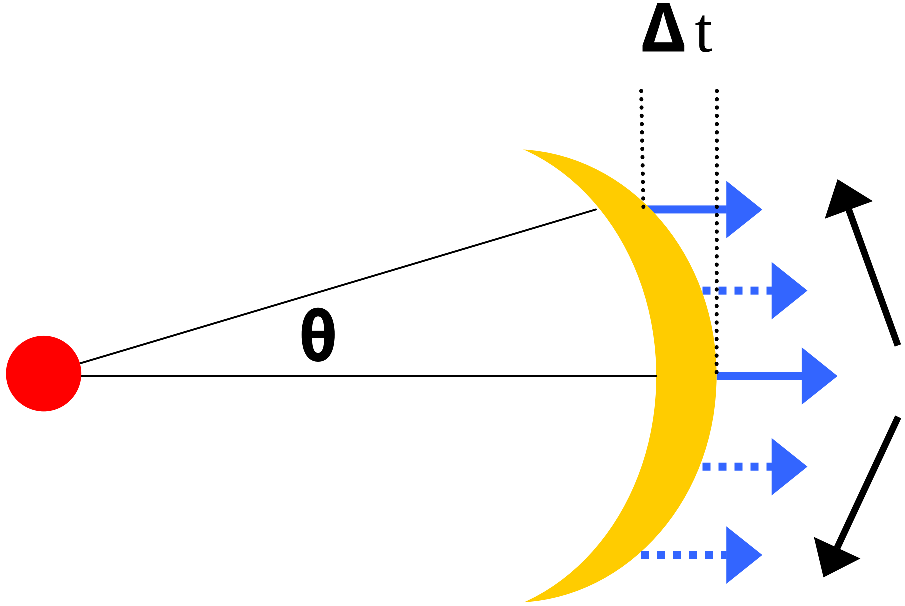

$$F_\nu \sim (t-t_0)^{-\alpha}\nu^{-\beta} \sim (t-t_0)^{-2-\beta}\nu^{-\beta}$$

$$\alpha = 2 + \beta$$

(Kumar & Panaitescu 2000)

α - β relation

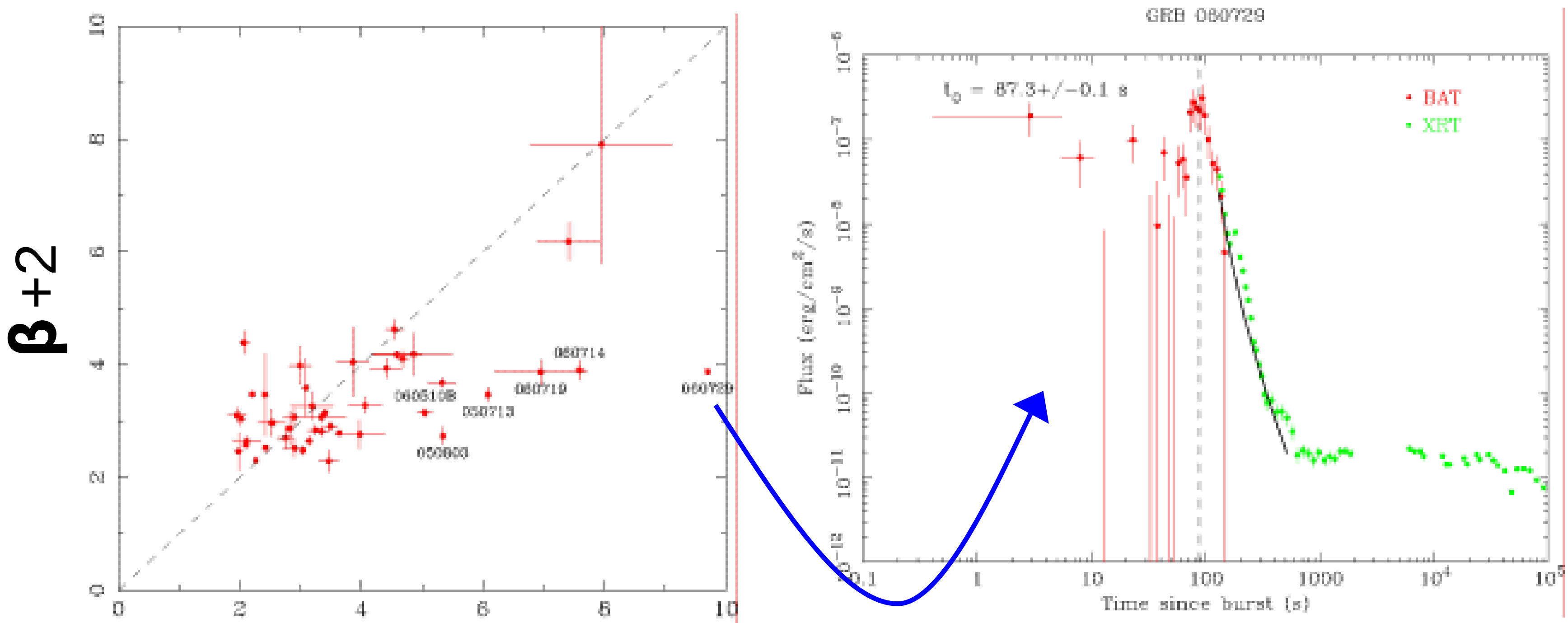

α (t_0 = trigger time)

α - β relation is satisfied in most cases, but some cases show a steeper temporal decay index (α > 2+ β).

We calculated the t_0 values by fitting the light curve with the function (Zhang et al. 2006, Liang et al. 2006)

$$F_\nu = A\,(t - t_0)^{-(2+\beta)} / t_0 + B\,t^{-C}$$

↓

t_0 values correspond to the beginning of the last pulse.

X-ray flares

X-ray flares

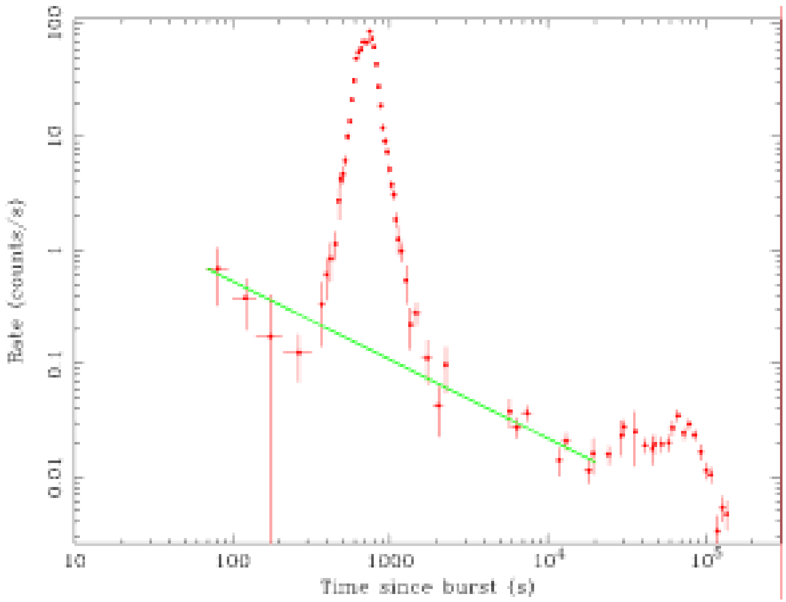

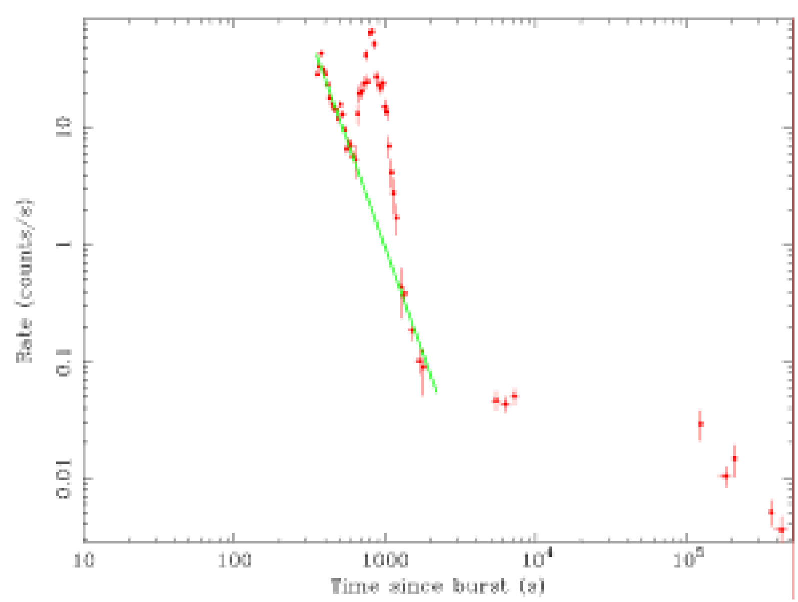

- X-ray flares show large amplitude and short timescale.
- Temporal decay index before and after the flare is approximately identical.

Afterglow (external shock) variability or not ?

Theoretical models of afterglow variability

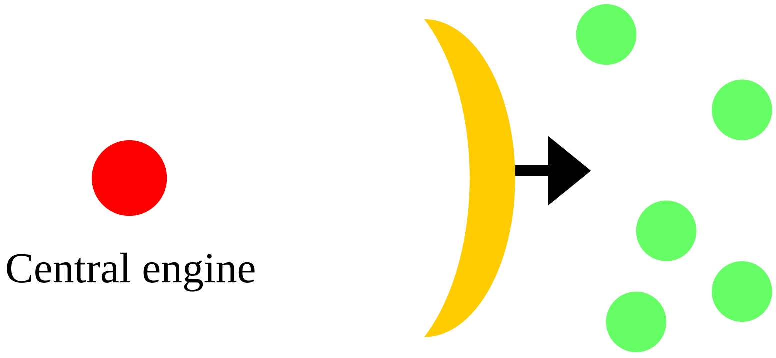

① Fluctuation in the ambient density

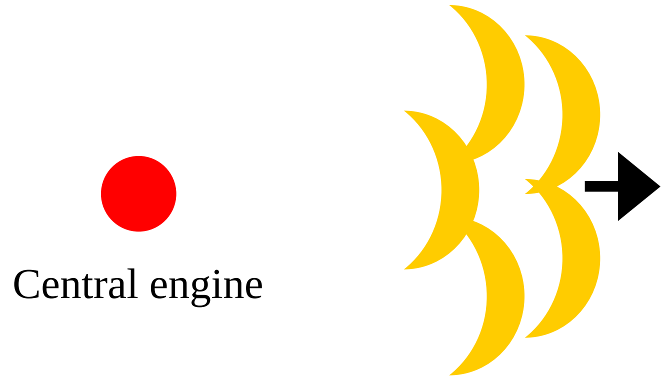

② Patchy shell model

③ Refreshed shock model

④ Long-acting engine model
(Internal shock model)

Kinematical limits on afterglow variability

Kinematical limits on afterglow variability
(Ioka et al. 2005)

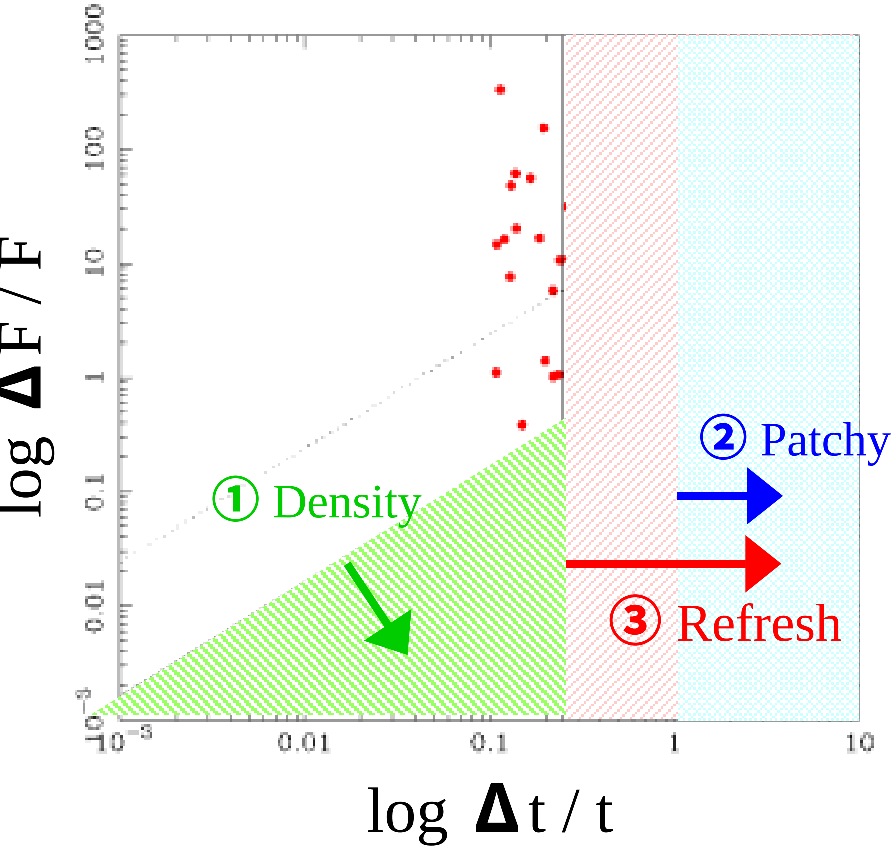

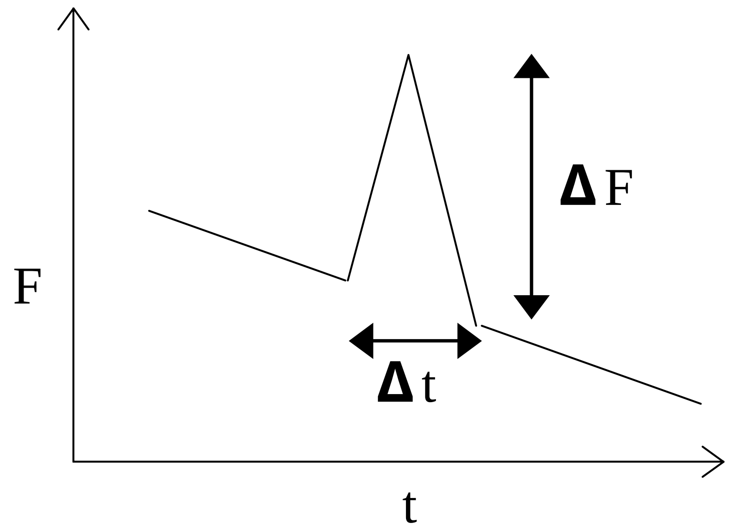

The X-ray flares with short time scale and large amplitude are difficult to explain with external shock.

Long-acting engine model
(Internal shock)

X-ray flare start time

We calculated the t_0 values of X-ray flares by assuming the α-β relation (Liang et al. 2006).

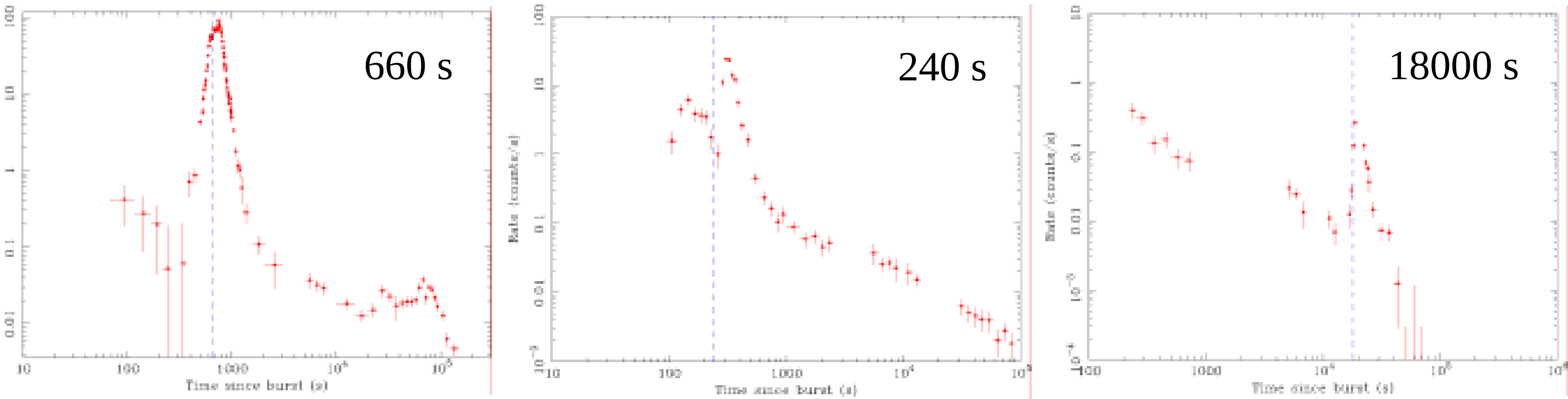

t_0 values are determined near the beginning of the rising segment of X-ray flares.

X-ray flares are due to central engine activity after the prompt emission is over.

Temporal profiles

Temporal profiles of GRB pulses are characterized by Norris et al. (1996).

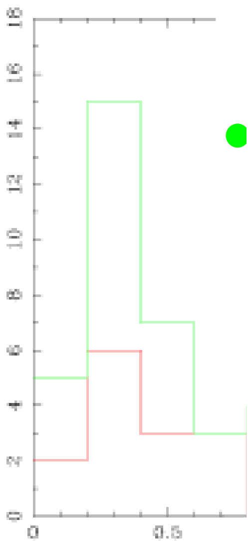

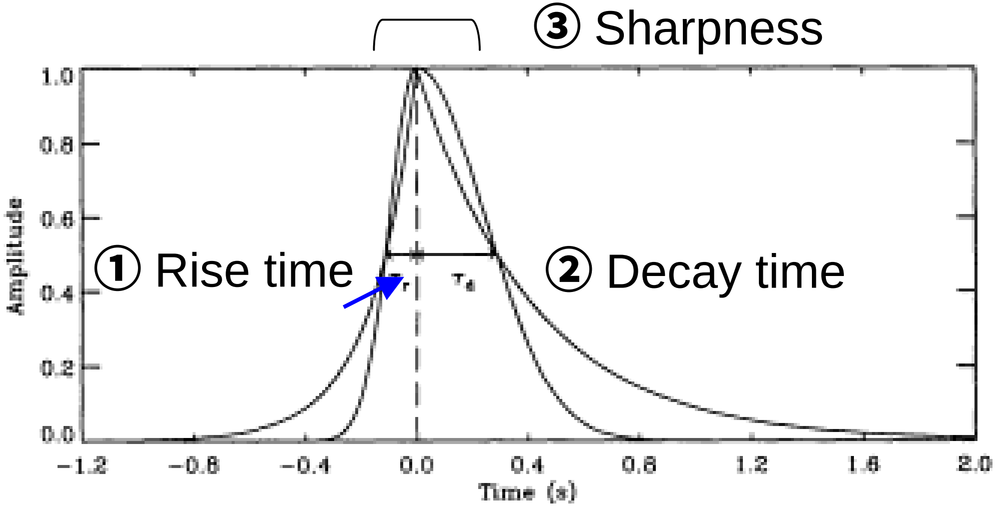

Norris et al. (1996)

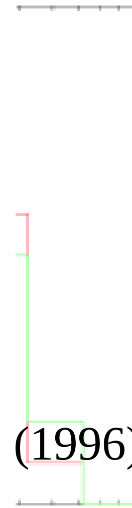

Rise tim

- F
- Pu
- Pu
  (sharpness ~ 1-2)

Pulse width $\Delta t \sim R/2c\gamma^2$

Small Lorentz factor of the shell or/and large emission radius

Spectral studies

We studied the spectral properties of individual X-ray flares using the XRT data (0.5-10 keV).

Best fit model : power-law ($\propto E^{-\Gamma}$)

- Photon index $\Gamma > 2.0$
  Spectral Peak energy is below the XRT energy band.
  $E_p < 0.5$ keV
- Photon index $\Gamma < 2.0$
  Spectral Peak energy is within or above the XRT energy band.
  $E_p \sim 0.5$-10 keV or $E_p > 10$ keV

We tried to fit the spectra using both the BAT and XRT data.

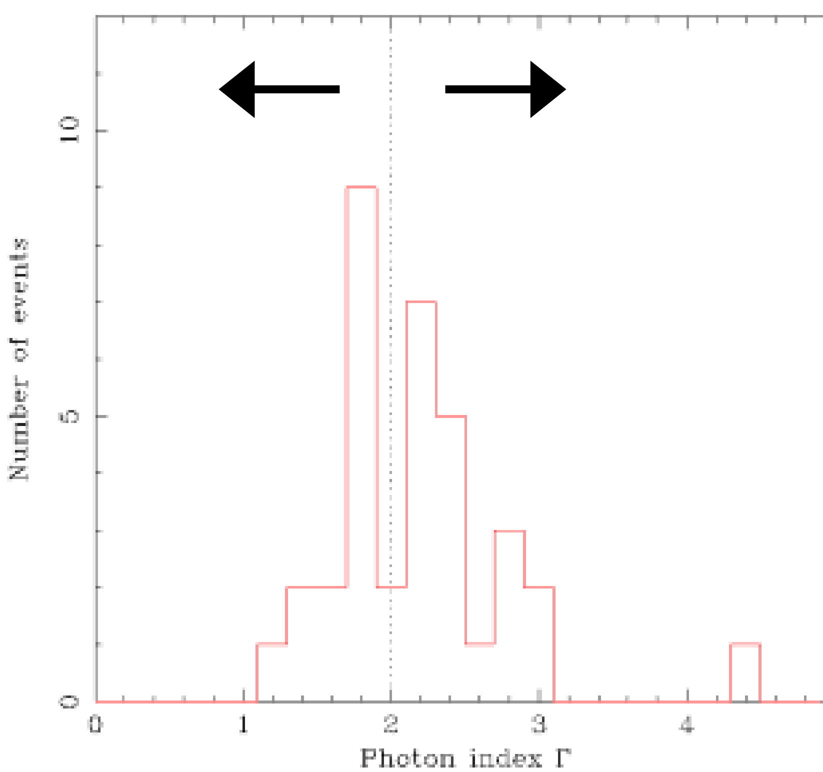

Distribution of the photon indices

BAT-XRT joint fit

We performed spectral fitting using both BAT and XRT data.
Best fit model

7 events : power-law (Γ < 2.0)

3 events : cutoff power-law or Band function

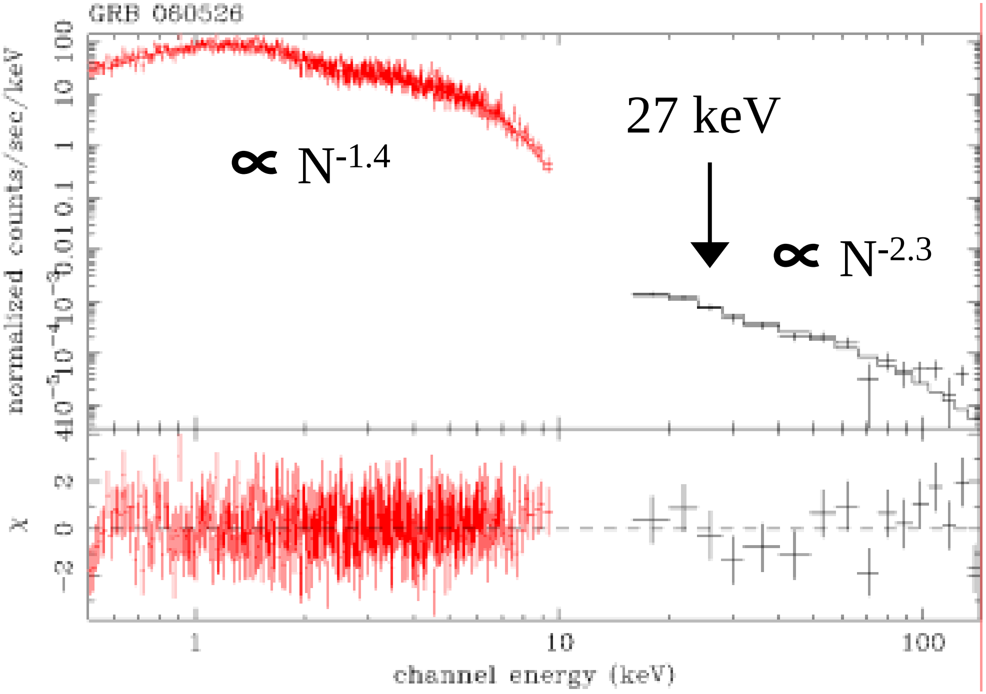

7 events were well fitted with PL (Γ <2.0)

Spectral peak energies are located above the BAT energy band.
E_p > 150 keV

E_p of X-ray flares are distributed 0.5~ few hundred keV.

Summary of X-ray flares

- X-ray flares with large amplitude and short timescale are difficult to explain with afterglow (external shock) models.
- T_0 of most X-ray flares are consistent with being near the beginning of the rising segment.
- Temporal profiles and spectral properties of X-ray flares and GRB have many common characteristics.

⇩

X-ray flares are likely due to central engine activity (internal shock scenario), after the GRB is over.

Shallow decay

Shallow decay

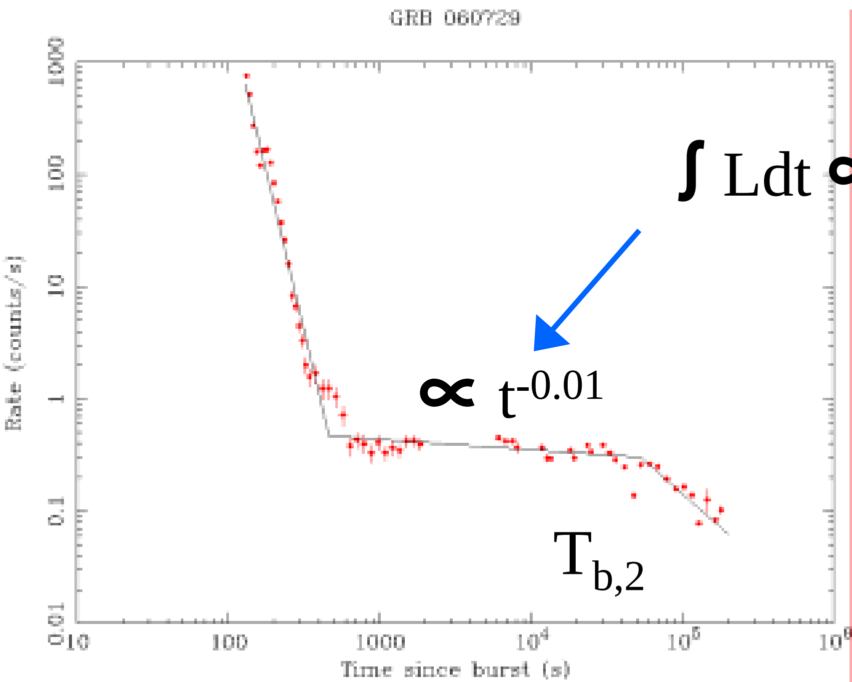

$\int L dt \propto \int t^{-0.5} dt \propto t^{0.5}$

Theoretical models of shallow decay
① Continuous energy injection model
② Inhomogeneous jet model
③ Time-dependent microphysics model

We examined if there are any correlation between the parameters of prompt emission and the shallow decay phase?

We compared the $E_{\gamma,iso}$ and the end time of the shallow decay phase $T_{b,2}$.

Estimation of the E_p

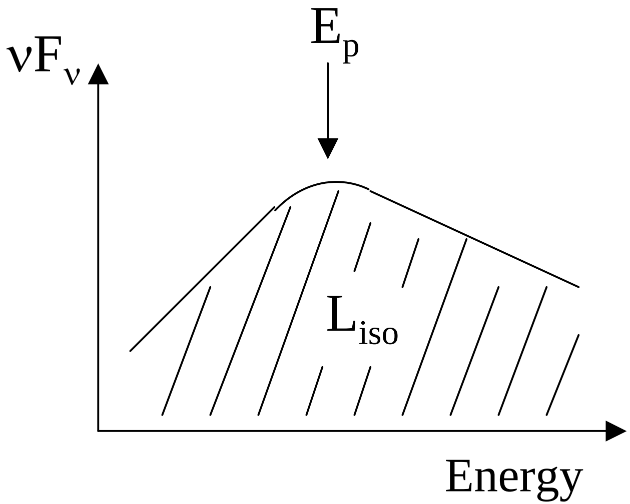

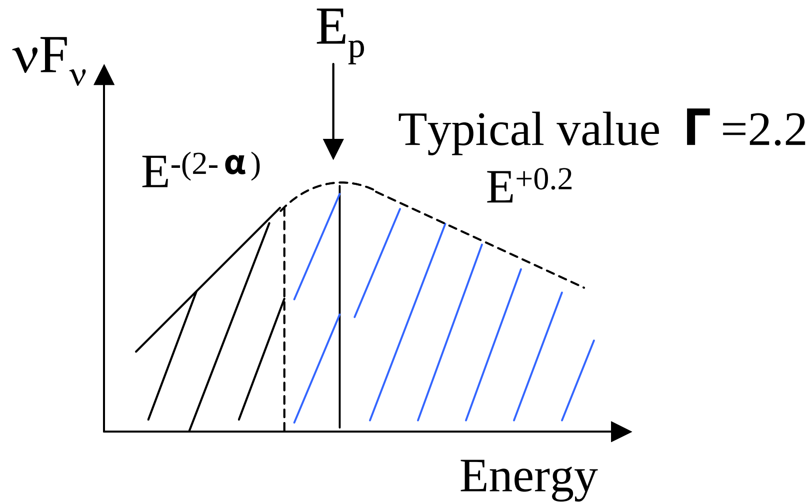

GRB spectrum typically described by a Band function.

BAT spectra are described by a PL. BAT cannot well determine Ep and high energy photon index.

Isotropic luminosity is estimated as

$$L_{iso} = 4\pi d_L^2 F_0 (1/(2-\alpha) - 1/(2-2.2)) E_p^{-\alpha}$$

$L_{iso} - E_p$ relation is given by Ghirlanda et al. (2005):

$$E_p / 100 \text{ keV} = 4.88 (L_{iso} / 1.9 \times 10^{52} \text{ erg/s})^{0.5}$$

We can obtain the E_p.

Correlation between $E_{\gamma,iso}$ and $T_{b,2}$

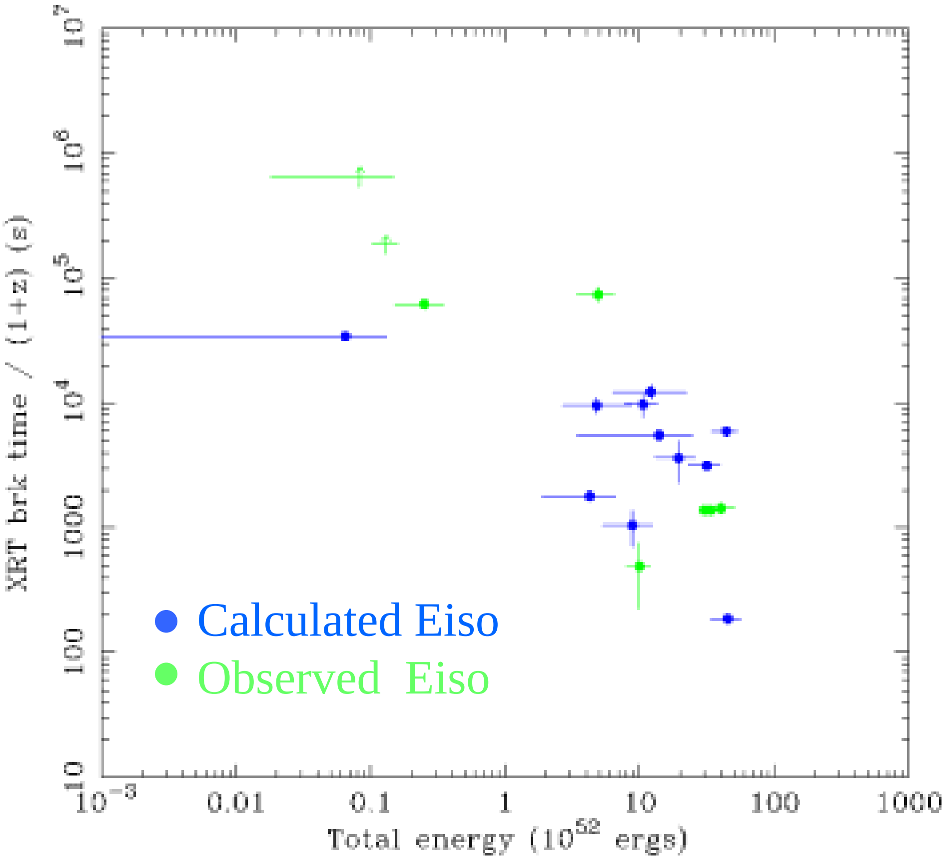

The larger the isotropic GRB energy ($E_{\gamma,iso}$),
the earlier the end time of shallow decay phase.

① Energy injection

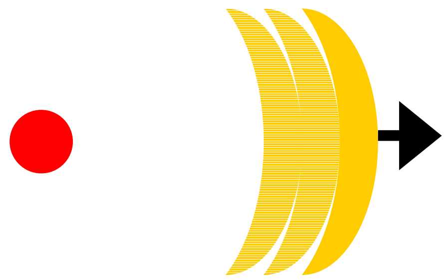

① Refreshed shock

The inner shell finishes to catch up with the outer shell at $T_{b,2}$.

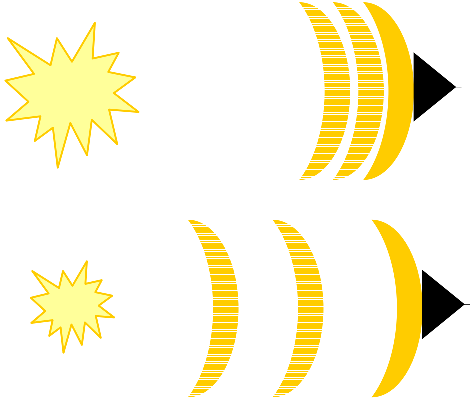

GRB with large $E_{\gamma,iso}$ eject shells with large Lorenz factors.

② Long-lived central engine

Central engine remains active until $T_{b,2}$.

X-ray flare model

- X-ray flares require episodic energy injectio

However,

- Shallow decay require smooth and continu energy inject n.

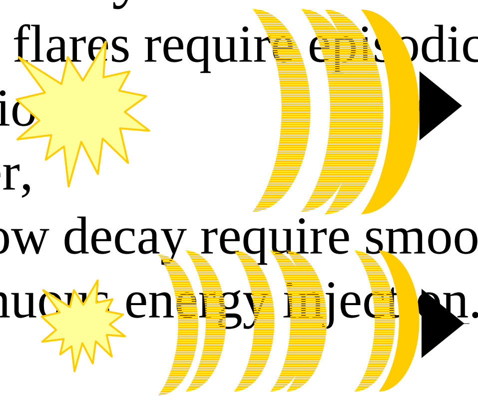

GRB with large $E_{\gamma,iso}$ eject shells more rapidly.

② Inhomogeneous jet

Toma et al. (2005)

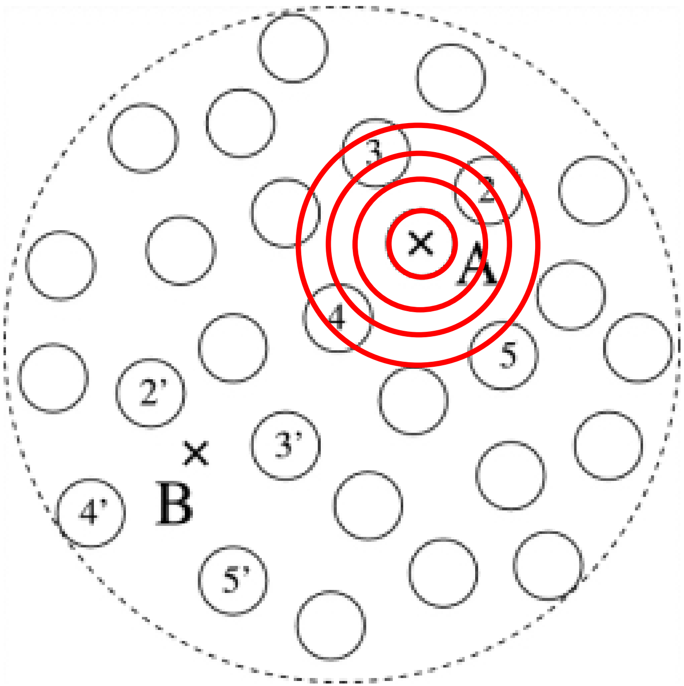

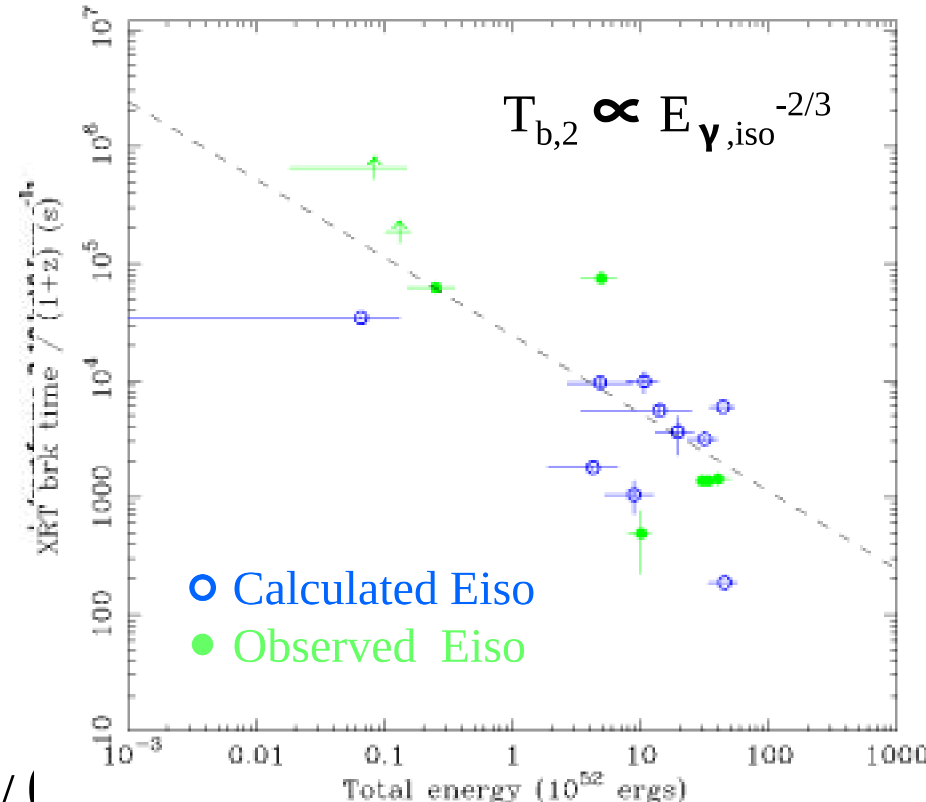

When the shell is decelerated to $\Gamma \sim 1/\theta$,
it begins to spread sideway.

⇩

Shallow decay phase

$T_{b,2} \propto E_{\gamma,iso}^{-2/3}$

③ Time-dependent microphysics

Energy fraction ε_B , ε_e depends on the shock's Lorentz factor Γ .

→ For $\Gamma > \Gamma_0$, ε_e、ε_B vary in the early afterglow.

For $\Gamma < \Gamma_0$, ε_e、ε_B are constant as observed in the late time afterglow.

(Γ_0 is the Lorentz factor of the outflow at the X-ray decline transition.)

$T_{b,2}$ corresponds to the time at which the Γ is decelerated to Γ_0.

Γ of the external shock evolves as $\Gamma(t) \propto E_{iso}^{1/8}\, t^{-3/8}$

↓

$T_{b,2} \propto \Gamma_0^{8/3} E_{\gamma,iso}^{1/3}$

Positive correlation between $T_{b,2}$ and $E_{\gamma,iso}$

⇩

This relation is inconsistent with the observational result of inverse correlation between $T_{b,2}$ and $E_{\gamma,iso}$.

Summary of shallow decay phase

From $E_{\gamma,iso} - T_{b,2}$ correlation,

- The shallow decay phase are likely not due to the “time-dependent microphysics model”.

However,

- “Energy injection model” and “Inhomogeneous jet model” have a serious problem.

  Unreasonably high gamma-ray efficiency of GRBs ≧ 75-90%
  (Toma et al. 2006, Ioka et al. 2006)

Conclusion

X-ray flares

- X-ray flares are likely due to “long central engine activity”.
- Temporal profiles and spectral properties of X-ray flares and GRB have many common characteristics.

Shallow decay phase

- The end time of the shallow decay phase is anti-correlated with $E_{\gamma,iso}$.

→ The shallow decay phase are likely not due to the “time-dependent microphysics model”.

However, other models “Energy injection model” and “Inhomogeneous jet model” have a serious problem.